- SUPPLEMENTARY MATERIAL -

Iron triggers λSo prophage induction and release of extracellular DNA in *Shewanella oneidensis* MR-1 biofilms

Lucas Binnenkade[a,b], Laura Teichmann[a], Kai Thormann[a,b]#

[a]*Max Planck Institute for terrestrial Microbiology, Marburg, Germany, Department of Ecophysiology*

[b]*Institute for Microbiology and Molecular Biology, Justus Liebig University Giessen, Germany*

Corresponding author; Mailing address:
Institut für Mikrobiologie und Molekularbiologie
Heinrich-Buff-Ring 26-32, 35392 Giessen, Germany
Tel.: +49(0)641 9935545, Fax: +49(0)641 9935549
email: kai.thormann@mikro.bio.uni-giessen.de

Table S1 Bacterial strains and plasmids

Bacterial strain or plasmid	Relevant genotype	Source or reference
Escherichia coli		
DH5α λpir	ϕ80d*lacZ*Δ*M15* Δ(*lacZYA-argF*)*U169 recA1 hsdR17 deoR thi-l supE44 gyrA96 relA1*/λpir	Miller and Mekalanos (1988)s
WM3064	*thrB1004 pro thi rpsL hsdS lacZ* ΔM15 RP4-1360 Δ(*araBAD*) 567Δ*dapA* 1341::[*erm pir*(wt)]	W. Metcalf, University of Illinois, Urbana-Champaign
***Shewanella oneidensis* MR-1**		
S79	wild type	Venkateswaran et al. (1999)
S176	*Tn7*::*ecfp*, tagged with *ecfp* in a mini-Tn7 construct	Gödeke *et al.* (2011b)
S198	*Tn7*::*egfp*, tagged with *ecfp* in a mini-Tn7 construct	Gödeke *et al.* (2011b)
S1387	ΔLambdaSo (SO_2939-SO_3013)	Gödeke *et al.* (2011b)
S1419	ΔLambdaSo ΔMuSo2 ΔMuSo1	Gödeke *et al.* (2011b)
S1393	S198 ΔLambdaSo (SO_2939-SO_3013)	Gödeke *et al.* (2011b)
S2933	Δ*λlysis-operon* (SO_2966-SO_2974)	This work
S2933	S198 Δ*λlysis-operon*	This work
S2391	*Tn7*::*ecfp* Pλ*cro*::*venus,* insertion of RBS and *venus-his6x* sequence downstream of putative λ*cro* (SO_2989) in strain S176	This work
S2502	Δ*recA* (SO_3430)	This work
S3173	*recA* complementation strain, insertion of *recA* wild type copy in S2502	This work
S2425	S2391, Δ*recA* (SO_3430)	This work
S2623	*Tn7*::*ecfp* PλR'::*venus,* insertion of RBS and *venus-his6x* sequence upstream of SO_2974 in strain S176	This work
S2395	*Tn7*::*ecfp* PλL::*venus,* insertion of RBS and *venus-his6x* sequence downstream of SO_2949 in strain S176	This work
S2991	Δ*oxyR* (SO_1328)	This work
S2989	Δ*fur* (SO_1937)	This work
S2993	S2391 Δ*oxyR* (SO_1328)	This work
S3065	S2391 Δ*fur* (SO_1937)	This work
S3104	*oxyR* complementation strain, insertion of *oxyR* wild type copy in S2993	This work
S3112	*fur* complementation strain, insertion of *fur* wild type copy in S3065	This work
S3169	Hydrogen peroxide-resistant strain, OxyR T104N substitution	This work
S3170	Hydrogen peroxide-resistant strain, OxyR L197P substitution	This work
S3171	OxyR T104N substitution in strain S2391	This work
S3172	OxyR L197P substitution in strain S2391	This work
Plasmids		
pNPTS138-R6KT	mobRP4$^+$ ori-R6K *sacB*; beta-galctosidase fragment alpha; suicide plasmid for in-frame deletions or integrations; Km^r	Lassak *et al.* (2010)
pNPTS138-R6KT- ΔrecA	Fragment for in-frame deletion of *recA* (SO_3430) in pNPTS138-R6KT; Km^r	This work
pNPTS138-R6KT- KIrecA	*recA* wild type gene copy for complementation by insertion into locus	This work
pNPTS138-R6KT- Δlysis-operon	Fragment for in-frame deletion of gene region SO_2939-SO_3013 (putative lysis operon) in pNPTS138-R6KT; Km^r	This work
pNPTS138-R6KT- ΔoxyR	Fragment for in-frame deletion of *oxyR* (SO_1328) in pNPTS138-R6KT; Km^r	This work
pNPTS138-R6KT- KoxyR	*oxyR* wild type gene copy for complementation by insertion into locus	This work
pNPTS138-R6KT- Δfur	Fragment for in-frame deletion of *fur* (SO_1937) in pNPTS138-R6KT; Km^r	This work
pNPTS138-R6KT- KI*fur*	*fur* wild type gene copy for complementation by insertion into locus	This work
pNPTS138-R6KT- Pλcro::RBS_venus-His6x	Fragment for insertion of RBS and venus-his6x sequence downstream of putative λ*cro* gene (SO_2989) in pNPTS138-R6KT; Km^r	This work
pNPTS138-R6KT- PλR'::RBS_venus-His6x	Fragment for insertion of RBS and venus-his6x sequence upstream of SO_2974 in pNPTS138-R6KT; Km^r	This work
pNPTS138-R6KT- PλL::RBS_venus-His6x	Fragment for insertion of RBS and venus-his6x sequence downstream of SO_2949 in pNPTS138-R6KT; Km^r	This work
pNPTS138-R6KT-KI-OxyR-T104N	Fragment for in-frame insertion of OxyR T104N construct (H_2O_2 resistance); Km^r	This work
pNPTS138-R6KT-KI-OxyR-L187P	Fragment for in-frame insertion of OxyR L187P construct (H_2O_2 resistance); Km^r	This work

pXVENC-2	Template vector for cloning of *venus* sequence; Km^r	M. Thanbichler, MPI, Marburg
pME6031-PmotB-lacZ	Constitutive expression of *lacZ*, *motAB* promoter fused to *lacZ*, Tc^R	Gödeke *et al.* (2011b)
pBBR1-MCS5-TT	Terminators *lambda T0* and *rrnB1 T1* cloned into pBBR1-MCS5, Gm^R	Gödeke *et al.* (2011a)
pBBR1-TT-MSC5-RBS-*venus*	Vector for promoter fusions, optimal RBS sequence upstream of venus gene, Gm^R	This work
pBBR1-TT-MSC5-Pdps-RBS-*venus*	Putative promoter region of *dps* (SO_1158) in pBBR1-TT-MSC5-RBS-*venus*, Gm^R	This work
pBBR1-TT-MSC5-PtonB-RBS-*venus*	Putative promoter region of *tonB* (SO_3670) in pBBR1-TT-MSC5-RBS-*venus*, Gm^R	This work
pBBR1-TT-Ptac-MCS5	Tac promoter region in pBBR1-MCS5-TT for constitutive expression, Gm^R	This work
pBBR1-TT-Ptac-MCS5-*sodB*	*sodB* (SO_2881) in pBBR1-TT-Ptac-MCS5, Gm^R	This work

Abbreviations: Km^R, kanamycin resistance; Tc^R, tetracycline resistance; Gm^R, gentamicin resistance

Table S2 Oligonucleotides used in this study

Name	Sequence (5'-3')	Enzyme
Knock-out/knock-in constructs		
EcoRI-KO_lysis-us-Fw	TCT ATG AAT TCC AAC CCA TCT AAC GAG AAT GCA GG	EcoRI
SalI-KO_lysis-ds-Rev	CTA GTC GAC GGC AGA TTT ATC GGC TGG AGC	SalI
Ol-KO_lysis-SO_2966-up-Rev	TAT GAA TAA GAC AGC GTG AAA CAA AAA AAC TCA CTT G	-
Ol-KO_lysis-SO_2974-ds-Fw	TTC ACG CTG TCT TAT TCA TAG ATG CCC CAA AAC AAA AAG	-
chk-KO_lysis_Fw	ATT GGC ACC GTA AGA GAT GGT GG	-
chk-KO_lysis_Rev	ATA AGC TTC TTG CGA GAC TAA ACC G	-
BamHI-drecA-us-fw	ATA GGA TCC GGC GTG TTG AAA TTG ATA AGG GA	BamHI
drecA-OL-us-rev	ATG AAG GTC GAT GGC GAA GTG TTC TGA GTC AGT C	-
drecA-OL-ds-fw	GAA CAC TTC GCC ATC GAC CTT CAT TCC TGT TCC C	-
SalI-drecA-ds-rev	CTA GTC GAC CCA CGG GCA GTG AGA GAA ATA CC	SalI
drecA-chk-fw	GTG GCG TAA AAG TGG TGG AAA CG	-
drecA-chk-rev	AGG GAA TGC CCG CCA TAG GG	-
NheI_KO_oxyR_Fw	ACT GCT AGC CAA TTG GTG CCG GTA CTC TAC T	NheI
US_KO_oxyR_Rev	ATT GTG CCG TTA AAT TTT TCA TTT TAT CGA TTG CCA C	-
DS_KO_oxyR_Fw	GAA AAA TTT AAC GGC ACA ATA ACT GAG TAT TTT GCC TG	-
SalI_KO_oxyR_Rev	ACT GTC GAC GCG ATT ATC GTT TTA GCC GCT TG	SalI
chk_oxyR_Fw	CCT AGA TCT CAA TAC ATT AGA ACA G	-
chk_oxyR_Rev	GTT GCC TCG ACT ACC CAC GC	-
PspOMI_KO_fur_Fw	ACT GGG CCC CAG TAA CCC TGC GAT GTT GA	PspOMI
US_KO_fur_Rev	GAC AGA TGG AAA CGA CGA ATA AGC TTG CTC GGC	-
DS_KO_fur_Fw	ATT CGT CGT TTC CAT CTG TCA TTG CTA ATC TCT TG	-
NheI_KO_fur_Rev	ACT GCT AGC CAA CCA ATA ACT GCC CAG AAA ACT C	NheI
chk_fur_Fw	CGA GCA GGA TGT TGA TGC CCT C	-
chk_fur_Rev	CCA GCA CGC TCA TGT AAA TCA TC	-
EcoRI_KO_oxyR_Rev	ACT GAA TTC GCG ATT ATC GTT TTA GCC GCT TG	EcoRI
Seq-oxyR-Fw	TCC ATA ACC TTA GTG GCA ATC G	-
Seq-oxyR-Rev	CCT TTA TAA GAC TCA CAA CAG GC	-
Venus insertions		
lambdaSo-cro-6xHis-OL-Rev	AAG CAT CAT CAT CAT CAT CAT TAA TTA ACT TAC GAA CAG GAT AAC	-
venus-6xHis-OL-Rev	TTA ATG ATG ATG ATG ATG ATG CTT GTA CAG CTC GTC CAT GCC GAG	-
lambdaSo-cro-RBS-OL-Fw	CTT GCT CAC CAT GTC AGT CCT CCT CTA GGC AAC TTG GTT TGA TTC	-
venus-RBS-OL-Fw	AGG AGG ACT GAC ATG GTG AGC AAG GGC GAG GAG	-
BamHI-lambdaSo-cro-US-Fw	ATA GGA TCC GCT GGA ATG GTA TGA ACG	BamHI
EcoRI-lambdaSo-cro-DS-Rev	TCT ATG AAT TCG AGT CTC AGC ATC AAT AG	EcoRI
lambdaSo-KLtail-6xHis-OL-Rev	AAG CAT CAT CAT CAT CAT CAT TAA AAG CAT TTT CCC GCC GTC AGC	-
lambdaSo-KLtail-RBS-OL-Fw	CTT GCT CAC CAT GTC AGT CCT CCT TTA ACG TAT TAG CCG CAC GCT	-
BamHI-lambdaSo-KLtail-US-Fw	ATA GGA TCC CTT GCT CGC CTT CCC ACC	BamHI
EcoRI-lambdaSo-KLtail-DS-Rev	TCT ATG AAT TCG GCC AGC GCA GTT AGA AG	EcoRI
chk-lambdaSo-cro-venus-Fw	GCG CTT CAT GCT CGA TTG CGG C	-
chk-lambdaSo-cro-venus-Rev	CAT AGA GGA TCT CAG CAG GTG TTA CG	-
chk-lambdaSo-KLtail-venus-Fw	CAG CGC TAC AAA TCC AGC CTT GGC	-
chk-lambdaSo-KLtail-venus-Rev	CCC GCG CGG ATT ATC CAT TGG C	-
venus-Strep-OL-Rev	GAT TTA TTT TTC GAA CTG CGG GTG GCT CCA GCC CTT GTA CAG CTC GTC CAT GCC GAG	-
lambdaSo-2974-RBS-OL-Fw	CTT GCT CAC CAT GTC AGT CCT CCT AGA TGC CCC AAA ACA AAA AGC	-
lambdaSo-2974-Strep-OL-Rev	TGG AGC CAC CCG CAG TTC GAA AAA TAA ATC ATG AAT AAG ATT TTG ATG AGT	-
EcoRI-lambdaSo-2974-US-Fw	TCT ATG AAT TCC CGT ATT GAT ACG TCC AAT CG	EcoRI

SalI-lambdaSo-2974-DS-Rev	CTA GTC GAC GAC TAA ACC GTA CTA GCG GCG GC	SalI
chk-PR'-SO_2974_venus-Rev	CCA CGC ATC GGA GAG GCT AAC C	-
chk-PR'-SO_2974_venus-Fw	GTG TAC TGG CGT GCA GCA AAT AAG C	-

Operon mapping

OM-2974-2975-Fw	GAT TAG TAA CAC TCA TCA AAA TCT TAT TC	-
OM-2974-2975-Rev	GGA ATT AAG GAT GAG TTT GGC CG	-
OM-2973-2974-Fw	ACC TTG GAT AAG ATG GCC ACG	-
OM-2973-2974-Rev	GTT GCA CAT GAT AAA AGT GAA TTA GC	-
OM-2972-2973-Fw	GCC AGC AAA TCA AGA CTG CCG	-
OM-2972-2973-Rev	CAT TGC TGT TGC CAG AGT ATC G	-
OM-2971-2972-Fw	GAA GAG TGC GAT TGT TGA TGC G	-
OM-2971-2972-Rev	CAG GTA TTC GAA AGG TCC AGC	-
OM-2970-2971-Fw	CTA TTT ACC AAG TGG CTG ATG GC	-
OM-2970-2971-Rev	GCG ATG ATT ATG GAT AAA GCA ACG	-
OM-2969-2970-Fw	CGT GGC AAT GCT TGC ACA GC	-
OM-2969-2970-Rev	CCA CTG GTA CCT GCT GAT TGG	-
OM-2968-2969-Fw	GAG TAC GCC CAT GTC TTT AAG C	-
OM-2968-2969-Rev	AGC GTG GTT ACG GTG GAC G	-
OM-2967-2968-Fw	ATC CTT CCA GCC GAA CAG CG	-
OM-2967-2968-Rev	AAC TTA CCA AAG CAT CAA AAT CAT CG	-
OM-2966-2967-Fw	GAC CAA CCA AGT CCA AAC AGG	-
OM-2966-2967-Rev	CAC TGT TTG AGA TAA AAA GCA TCG G	-
OM-2965-2966-Fw	AAG TCG ATA TCC ATG CGG TGC	-
OM-2965-2966-Rev	TGG TCG CTG TTA TCT GGT TCG	-
OM-2964-2965-Fw	GCC TGG GGA ATT GAT ATA AAC GG	-
OM-2964-2965-Rev	ACA ACG GCA AAC CCA ATA CGC	-
OM-2963-2964-Fw	CTC ACC GAT TGA CTG CTC GC	-
OM-2963-2964-Rev	AGC CGA TGA AAT TGG TGA GAC C	-
OM2-2968-2969-Fw	CAT GCG GCT TTG GCT CTT GGG	-
OM2-2968-2969-Rev	CTT CTT AAA GCG CAA TCC TCT CTG C	-
OM2-2970-2971-Fw	CGT TGG TTT GGG CAG TAA TGG C	-
OM2-2970-2971-Rev	GCT ATG TCG CTT CAA TCT CTA CGG	-

Promoter fusion studies (pBBR1-TT-MSC5-RBS-venus)

PspOMI_pXVENC-2_RBS_Venus_Fw	ACT GGG CCC AGG AGG GCA AAT ATG GTG AGC AAG GGC GAG GAG	PspOMI
KpnI_pVENC-2_Venus_Rev	ACT GGT ACC TTA CTT GTA CAG CTC GTC CAT GCC	KpnI
EcoRI_PtonB_Fw	ACT GAA TTC ACC CGT AAC AGT CAT TCG CCC	EcoRI
PspOMI_PtonB_Rev	ACT GGG CCC GGC AAA CCT TCC AAT TCC AAA AGC	PspOMI
BamHI_Pdps_Fw	ACT GGA TCC AGG GTT AAT AGG ATT TTC ACT GG	BamHI
EcoRI_Pdps_Rev	ACT GAA TTC TCC TCC TAT TGT CCT ACT CGA TG	EcoRI
***sodB* over-expression**		
XhoI-RBS-sodB-Fw	TAT CTC GAG AGG AGG GCA AAT ATG GCT TTC GAA TTA CCC GCA TTA CC	XhoI
KpnI-sodB-Rev	CTG GGT ACC TTA ACC TGC GAA GTT TTG GTT CAC G	KpnI

Quantitative real-time PCR

katB-qPCR-Fw	CAC TTC AAA TCG CAG CAA GGC G	-
katB-qPCR-Rev	GGC ATG ATC TGC ACA TTC ACC G	-
dps-qPCR-Fw	TGG CAT AGG CTG AAT AGG AGC C	-
dps-qPCR-Rev	CGT CAC TGG TCC TAT GTT CAC C	-

katG1-qPCR-Fw	ATC TAC CGC GAA ATC ACC ACG C	-
katG1-qPCR-Rev	CTT GCC AAA TCA GTG CTT CGG C	-
ahpC-qPCR-Fw	TCA CGA AAG TAC CAC GCA GTG C	-
ahpC-qPCR-Rev	CAT GGC ACG ATA CTT CTG ACA CC	-
tonB-qPCR-Fw	TCG CAG GAG CAT CAC TAC ACC	-
tonB-qPCR-Rev	AAC CAC GGT TTG ATG AGG CGC	-
16s-rRNA-qPCR-Fw	AGG TTC ATC CAA TCG CGA GAG G	-
16s-rRNA-qPCR-Rev	GTT TAC TCA TGA GGT GGC GAG C	-
recA-qPCR-Fw	TCA CAT CAA CCG CAC CAG AAC G	-
recA-qPCR-Rev	CGC TCT TGA TCC TAT CTA CGC G	-

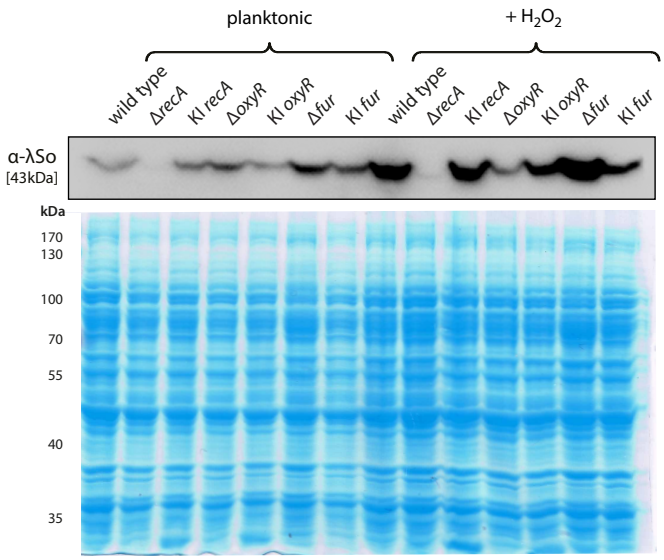

Figure S1. Western immunodetection of phage λSo in in-frame deletion strains and complementation strains in the absence and presence of H_2O_2. The strains were grown until mid-logarithmic phase in plain LM medium (+15 mM lactate) and then incubated with (LM+ H_2O_2) or without (LM) 2 mM H_2O_2 for 3h hours at 30°C and then subjected to SDS-PAGE and immunodetection. Δ, in-frame deletion; KI, in-frame reinsertion/knock-in.

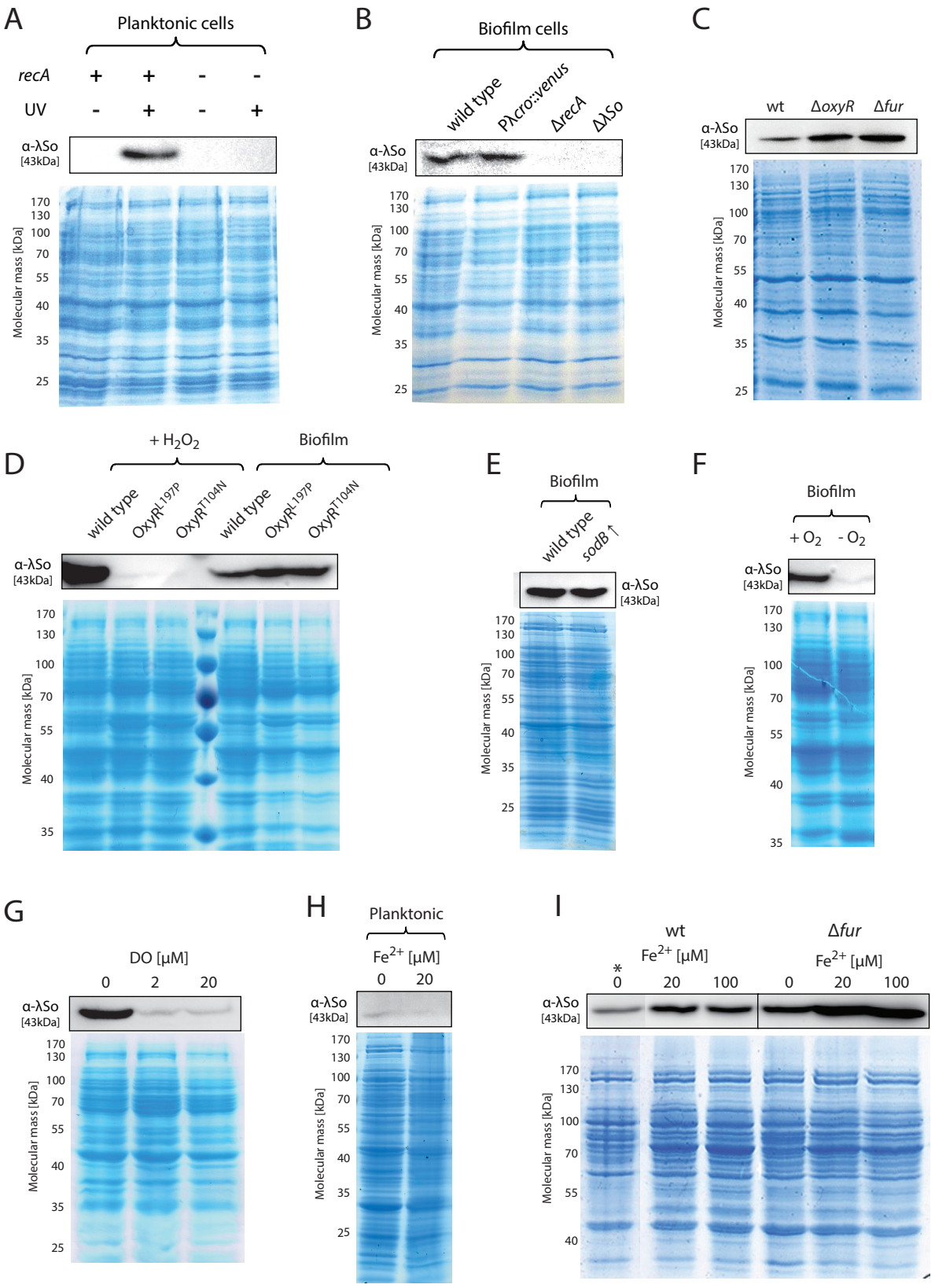

Figure S2. SDS-PAGE loading controls for λSo Western immunodetection assays. For each analysis, one SDS-PAGE gel was stained with Roti-Blue for visual analysis. Depicted are SDS-PAGE loading controls for Figure 2A **(A)**, Figure 2C **(B)**, Figure 3A **(C)**, Figure 4C **(D)**, Figure 4D **(E)**, Figure 4E **(F)**, Figure 5D **(G)**, Figure 5E **(H)** and Figure 5F,G **(I)**. *Lane 1 (wild type without additional ferrous iron) was located elsewhere on the same gel/blot and was copied next to the other lanes for direct comparison.

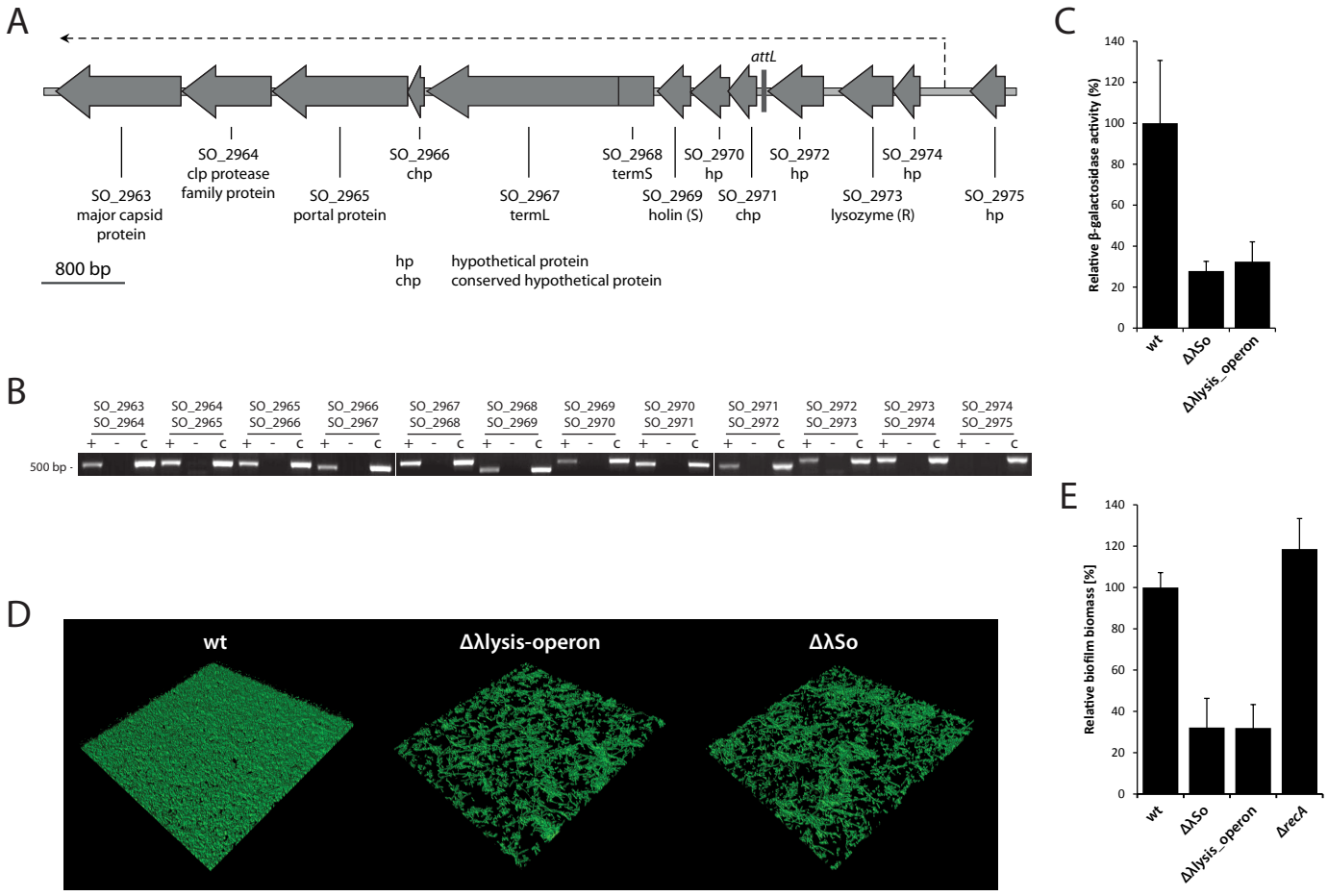

Figure S3. λSo prophage-mediated lysis is required for normal biofilm formation. (A) Genetic and transcriptomic organization of cluster SO_2963 to SO_2975. Predicted genes are indicated as grey arrows. Gene transcription starts at gene SO_2974 and continues at least until gene SO_2963, as indicated by RT-PCR analysis. Bioinformatic predictions are based on NCBI BLAST (National Library of Medicine) and PHAST (6) analyses. **(B)** Operon mapping using RT-PCR on genes SO_2963 to SO_2975 on cDNA samples (+) using appropriate primer pairs bracketing the gaps between the genes of interest. A corresponding total-RNA (-) sample taken before reverse transcription served as negative control, and chromosomal DNA (c) served as positive control. The PCR products were analyzed by 2% agarose gel electrophoresis. PCR amplification products were obtained for all genes except SO_2974 and SO_2975, indicating that that genes SO_2966 to SO_2974 reside on a single transcript. **(C)** Relative extracellular β-galactosidase activity of strain S2933 (Δλlysis-operon) and S1387 (ΔλSo) in comparison to the wild type. All strains harbored plasmid pME6031-PmotB-lacZ for constitutive cytoplasmic expression of β-galactosidase. Black bars represent mean values of biological and technical triplicates with standard deviations. Lysis was suppressed to a similar degree as in a λSo deletion mutant, indicating that deletion of gene cluster SO_2966 to SO_2974 is sufficient to completely suppress λSo-mediated cell lysis **(D)** CLSM projections of 24 hours-old biofilms formed by the wild type, the lysis operon deletion mutant (Δλlysis-operon) and the λSo prophage deletion mutant ΔλSo under hydrodynamic conditions in flow cells. All strains were tagged with Gfp. The lateral edge of each micrograph is 250 µm. The results indicate that a mutant lacking the λSo lysis-operon displays a biofilm-deficient phenotype highly similar to that observed for a complete λSo deletion. (E) Relative biomass as a measure of total fluorescence compared to the wild type of 24 hours-old biofilms formed by strain ΔλSo (relative Gfp values), Δλlysis_operon (relative Gfp values) and strain Pλ*cro::venus* Δ*recA* (relative Cfp values) under hydrodynamic conditions in flow cells. Bars represent the mean values (in %) with standard deviations displayed as error bars, obtained from two independent experiments conducted at least in duplicates.

Prophage λSo (*S. oneidensis* MR-1)

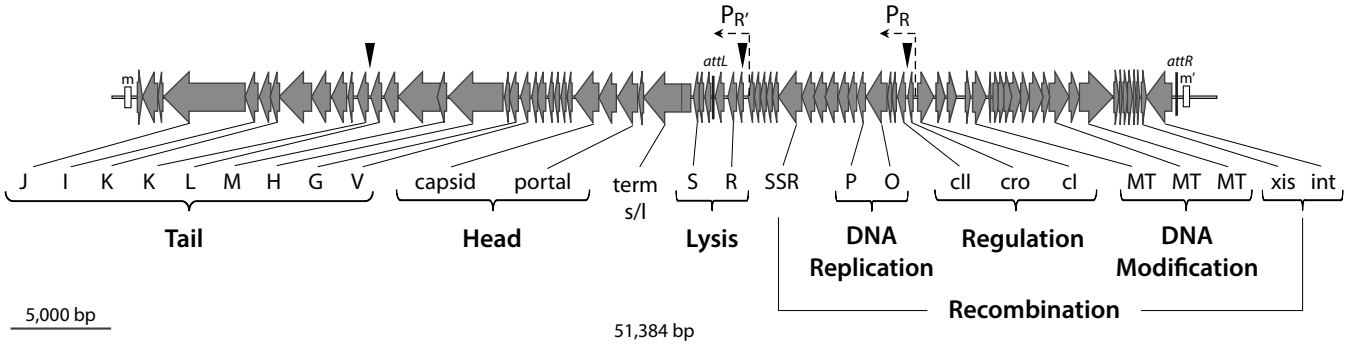

Figure S4. Genetic organization of prophage λSo and site-specific transcriptional fusion constructs. Predicted genes are indicated as grey arrows. Gene nomenclature is based on homologies to *E. coli* phage Lambda. Abbreviations for predicted putative genetic elements: m/m', cohesive ends (*cos* sites); *attL/R*, attachment sites; terms/terml, small and large subunit of phage terminase; SSR, Site-specific recombination protein; MT, methyltransferase; P_R, promoter for early transcription; $P_{R'}$, promoter for late transcription. Black arrows indicate the integration site for *venus* constructs used for transcriptional fusion to genes *cro*, promoter $P_{R'}$, and gene L.

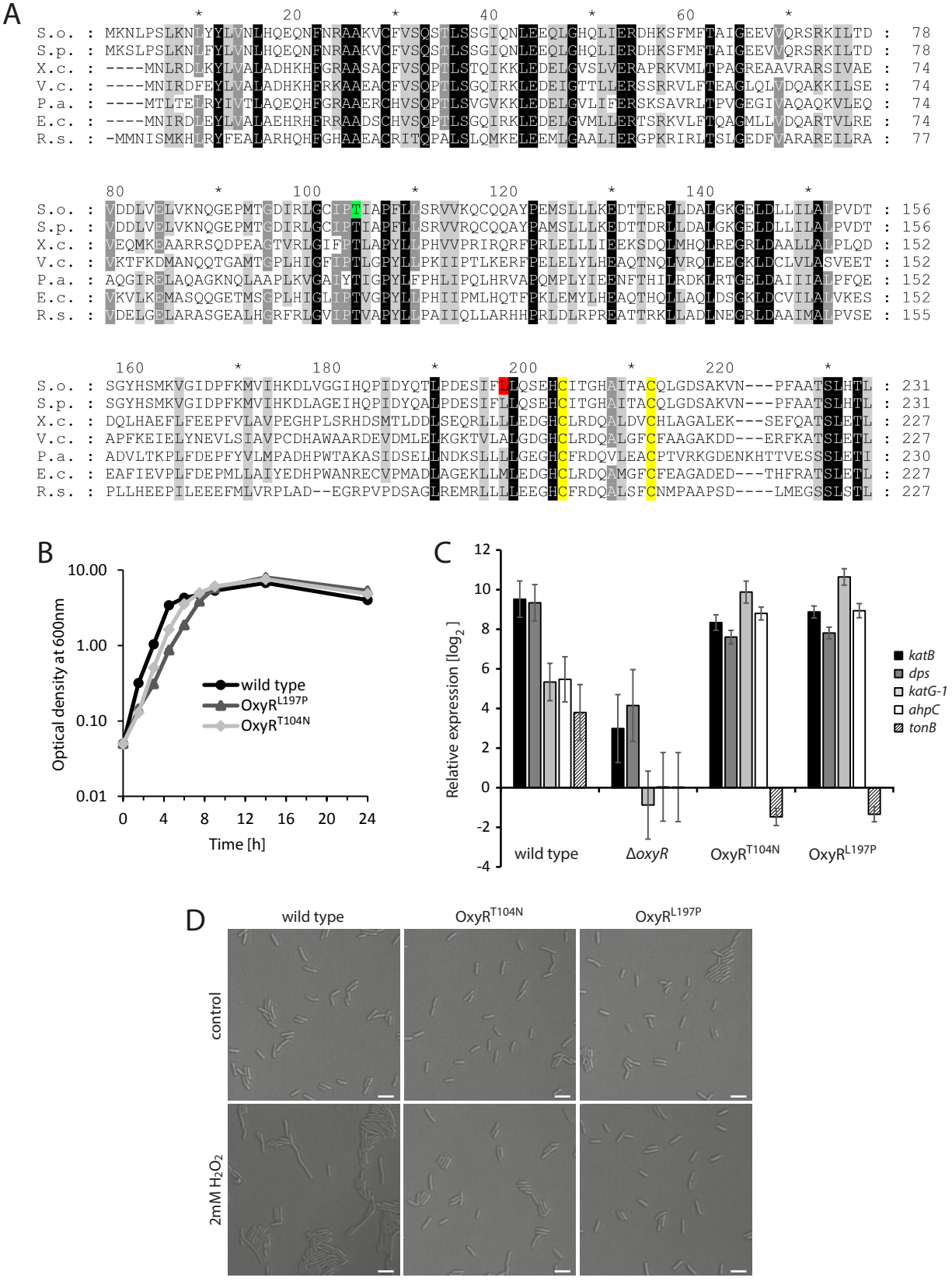

Figure S5. Characterization of H_2O_2 resistant mutants OxyR^{T104N} and OxyR^{L197P}. (A) Alignment of OxyR protein sequences of *S. oneidensis* MR-1 (S.o.), *S. putrefaciens* CN-32 (S.p.), *Xanthomonas campestris* (X.c.), *Vibrio cholera* (V.c.), *Pseudomonas aeruginosa* PAO1 (P.a.), *Escherichia coli* (E.c.), and *Rhodobacter sphaeroides* (R.s.). Protein sequences were aligned by ClustalW2 (EMBL-EBI) using standard slow pairwise alignment options. Grey and black background colors highlight highly conserved amino acid residues. Green highlights the T104N amino acid substitution, red the L197P amino acid substitution, and yellow highlight conserved cysteine residues for disulfide bond formation under oxidizing conditions. **(B)** Planktonic growth under aerobic conditions in LB medium of the *S. oneidensis* MR-1 wild type and the OxyR^{T104N} and OxyR^{L197P} mutant strains. Growth curves are derived from a representative experiment conducted in triplicates. Error bars represent standard deviations **(C)** Relative expression to the wild type in response to 2 mM H_2O_2 (15 min) of *katB* (SO_1070), *dps* (SO_1158), *ahpC* (SO_0958), *katG-1* (SO_0725) and *tonB* (SO_3670) in the Δ*oxyR* and the OxyR^{T104N} and OxyR^{L197P} mutant strains, determined by quantitative real-time PCR. Bars represent the mean values of two independent experiments, each normalized to the 16s rRNA and *recA* house-keeping genes. Standard deviations are displayed as error bars **(D)** Cell morphologies of the *S. oneidensis* MR-1 wild type and the H_2O_2 hyper-resistant mutants after exposure to 2mM H_2O_2 for 2 hours. The scale bar is 5 µm.

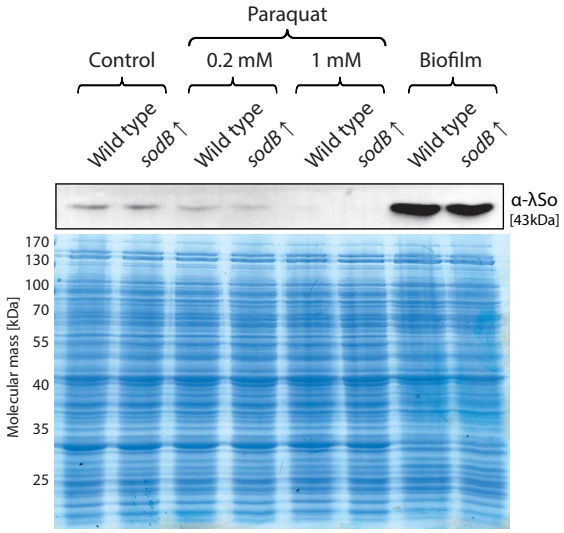

Figure S6. Western immunodetection of phage λSo in the wild type and a wild type strain carrying plasmid pBBR1-TT-Ptac-MCS5-*sodB* for constitutive overexpression of the *sodB* gene (SO_2881) in the absence or presence of 0.2 mM / 1 mM paraquat. The strains were grown until mid-logarithmic phase in plain LM medium (+15 mM lactate), incubated with or without paraquat for 3h hours at 30°C and finally harvested and subjected to SDS-PAGE and immunodetection. Samples of both strains grown under hydrodynamic biofilm conditions were additionally included for direct comparison.

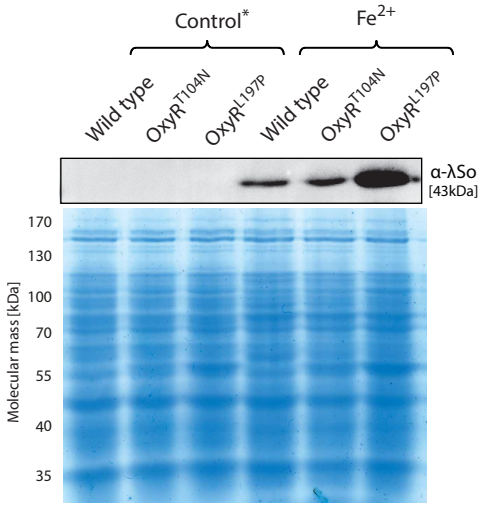

Figure S7. Western immunodetection of phage λSo in biofilm cells of the wild type and the OxyR^{T104N} and OxyR^{L197P} mutant strains cultivated under static conditions in LM medium without (control) and with 20 µM additional Fe^{2+}. The corresponding SDS-PAGE gel (stained) is illustrated as loading control. *no bands visible in the control samples due to the short exposure time that was necessary to avoid over-exposure of the Fe^{2+} treated samples

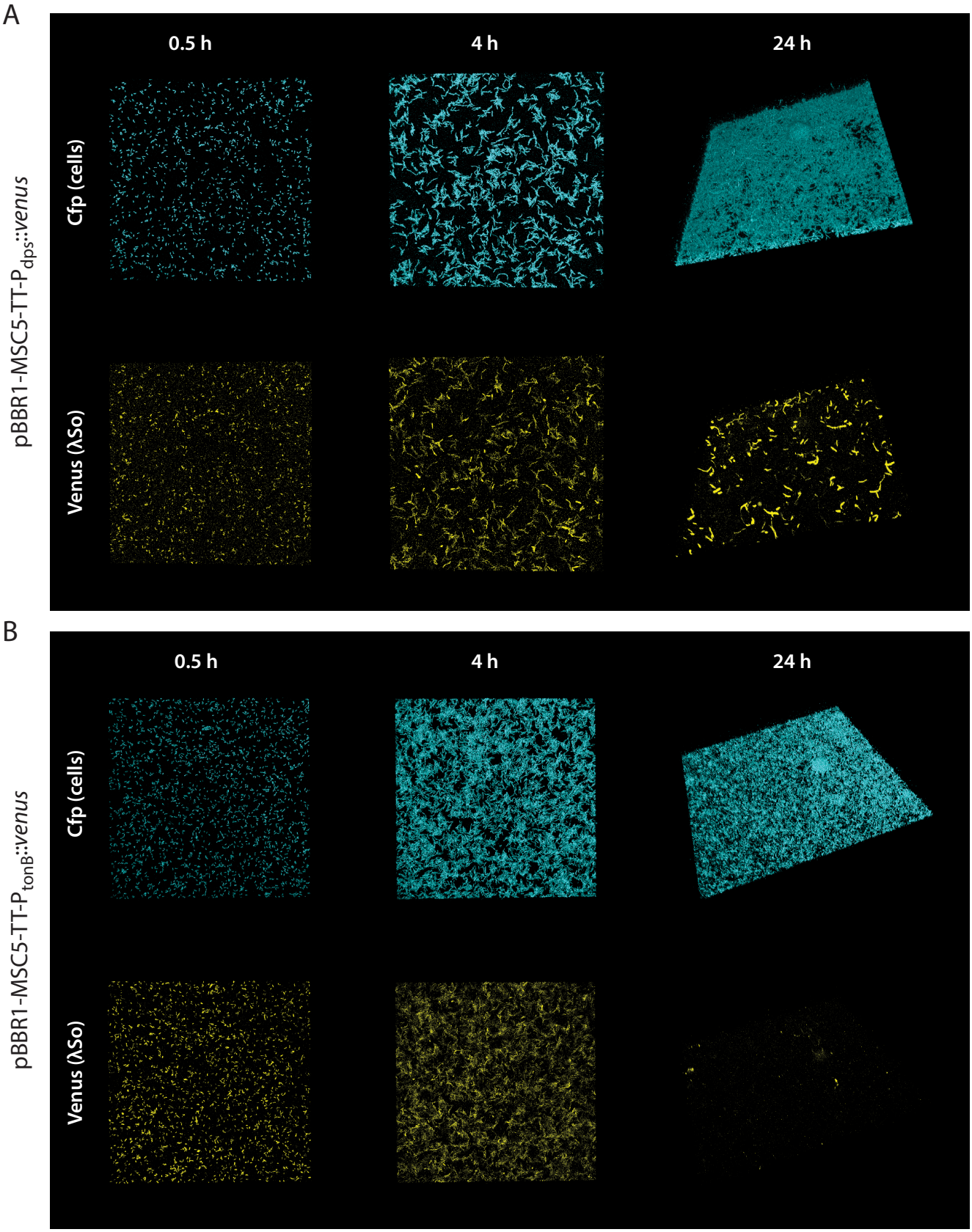

Figure S8. Activity of promoter P_{tonB} (A) and P_{dps} (B) during biofilm development. Displayed are CLSM images of 24 hours-old biofilms formed by Cfp-tagged *S. oneidensis* MR-1 wild-type strains harboring plasmid pBBR1-MSC5-TT-P_{tonB}::*venus* or plasmid pBBR1-MSC5-TT-P_{tonB}::*venus* under hydrodynamic conditions in flow cells. Venus fluorescence is expected to positively correlate with promoter activity. The lateral edge of each micrograph is 250 µm.

Additional references

1. **Miller VL, Mekalanos JJ.** 1988. A novel suicide vector and its use in construction of insertion mutations: osmoregulation of outer membrane proteins and virulence determinants in *Vibrio cholerae* requires *toxR*. J Bacteriol **170:**2575-2583.

2. **Venkateswaran K, Moser DP, Dollhopf ME, Lies DP, Saffarini DA, MacGregor BJ, Ringelberg DB, White DC, Nishijima M, Sano H, Burghardt J, Stackebrandt E, Nealson KH.** 1999. Polyphasic taxonomy of the genus *Shewanella* and description of *Shewanella oneidensis* sp. nov. Int J Syst Bacteriol **49 Pt 2:**705-724.

3. **Lassak J, Henche AL, Binnenkade L, Thormann KM.** 2010. ArcS, the cognate sensor kinase in an atypical Arc system of *Shewanella oneidensis* MR-1. Appl Environ Microbiol **76:**3263-3274.

4. **Gödeke J, Paul K, Lassak J, Thormann KM.** 2011. Phage-induced lysis enhances biofilm formation in *Shewanella oneidensis* MR-1. ISME J **5:**613-626.

5. **Gödeke J, Heun M, Bubendorfer S, Paul K, Thormann KM.** 2011. Roles of two *Shewanella oneidensis* MR-1 extracellular endonucleases. Appl Environ Microbiol **77:**5342-5351.

6. **Zhou Y, Liang Y, Lynch KH, Dennis JJ, Wishart DS.** 2011. PHAST: a fast phage search tool. Nucleic Acids Res **39:**W347-352.